1   **Hydrogeochemical Controls on Brook Trout Spawning Habitat in a Coastal Stream**
2

4   Martin A. Briggs[1*], mbriggs@usgs.gov, (phone) +1.860.487.7402

5   Judson W. Harvey[2]

6   Stephen T. Hurley[3]

7   Donald O. Rosenberry[4]

8   Timothy McCobb[5]

9   Dale Werkema[6]

10   John W. Lane, Jr.[1]

12   [1]U.S. Geological Survey, Hydrogeophysics Branch, 11 Sherman Place, Unit
13   5015, Storrs, CT, 06269 USA

14   [2]U.S. Geological Survey, Water Cycle Branch, M.S. 430, Reston, VA, 20192
15   USA

16   [3]Massachusetts Division of Fisheries and Wildlife, 195 Bournedale Road,
17   Buzzards Bay, MA, 02532 USA

18   [4]U.S. Geological Survey, National Research Program, M.S. 406, Bldg. 25, DFC,
19   Lakewood, CO, 80225 USA

20   [5]U.S. Geological Survey, 10 Bearfoot Road, Northborough, MA, 01532 USA

21   [6]U.S. Environmental Protection Agency, Office of Research and Development,
22   National Exposure Research Laboratory, Exposure Methods & Measurement
23   Division, Environmental Chemistry Branch, Las Vegas, NV, 89119 USA

34   Re-revised manuscript prepared for submission to *Hydrology and Earth Systems Sciences*

Abstract:

Brook trout (*Salvelinus fontinalis*) spawn in fall, and overwintering egg development

can benefit from stable, relatively warm temperatures in groundwater seepage zones. However,

eggs also are sensitive to dissolved oxygen concentration, which may be reduced in discharging

groundwater (i.e. seepage). We investigated a 2-km reach of the coastal Quashnet River, Cape

Cod, Massachusetts, USA, to relate preferred fish spawning habitat to geology, geomorphology,

and discharging groundwater geochemistry. Thermal reconnaissance methods were used to

locate zones of rapid groundwater discharge, which were predominantly found along the center

channel of a wider stream valley section. Pore-water chemistry and temporal vertical

groundwater flux were measured at a subset of these zones during field campaigns over several

seasons. Seepage zones in open valley sub-reaches generally showed suboxic conditions and

higher dissolved solutes compared to the underlying glacial outwash aquifer. These discharge

zones were cross-referenced with preferred brook trout redds, evaluated during 10 yr of

observation, all of which were associated with discrete alcove features in steep cut banks where

stream meander bends intersect the glacial valley walls. Seepage in these repeat spawning zones

was generally stronger and more variable than open valley sites, with higher dissolved oxygen

and reduced solute concentrations. The combined evidence indicates that regional groundwater

discharge along the broader valley bottom is predominantly suboxic due to the influence of near-

stream organic deposits; trout show no obvious preference for these zones when spawning.

However, the meander bends that cut into sandy deposits near the valley walls generate strong,

oxic seepage zones that are utilized routinely for redd construction and the overwintering of trout

eggs. Stable water isotopic data support the conclusion that repeat spawning zones located

directly on preferential discharges of more localized groundwater. In similar coastal systems

with extensive valley peat deposits, specific use of groundwater discharge points by brook trout

59   may be limited to morphologies such as cut banks where groundwater flowpaths do not

60   encounter substantial buried organic material and remain oxygen rich.

Introduction

61

62   The heat tracing of waters can be used to map a distribution of spatially focused, or

63   "preferential", groundwater discharge zones throughout surface water systems at times of

64   contrast between surface and groundwater temperature. The measurement of water temperature

65   from the reach to watershed scale is now possible using thermal infrared and fiber-optic

66   distributed temperature sensing (FO-DTS) methodology (Dugdale, 2016; Hare et al., 2015; Steel

67   et al., 2017). Remote infrared data collection throughout the river corridor has been enabled by

68   handheld cameras, piloted aircraft, and the rapidly evolving capabilities of unmanned aerial

69   systems. Researchers are capitalizing on the ongoing refinement of these technologies to

70   identify zones of focused groundwater seepage to streams to map potential discrete preferential

71   coldwater fish habitat such as summer thermal refugia (Dugdale et al., 2015). However, surface

72   thermal surveys alone do not indicate groundwater flowpath dynamics or the suitability of

73   interface aquatic habitat (Briggs et al., 2018a).

74   For example, dissolved oxygen (DO) concentration must be sufficiently high for cold

75   groundwater seepage to provide support for fish life-processes at the direct point of discharge to

76   surface water (Ebersole et al., 2003), which is not apparent from thermal analysis alone. During

77   summer warm periods in systems with suboxic groundwater, coldwater fish species such as

78   salmonids can face a tradeoff between occupying discrete zones of preferred water temperatures

79   with near-lethal DO levels, or stream sections that are too warm for long-term survival

80   (Matthews and Berg, 1997). The use of groundwater upwelling zones as thermal refugia is

81   further complicated by competition with aggressive invasive species (to the northeastern USA)

82   such as brown trout that compete with native trout for resources (Hitt et al., 2017). Streams at

83   higher elevations may support the persistence of reach-scale cold water habitat where point-scale

84   thermal refugia are not needed under current climatic conditions, serving as vital "climate

85   refugia" against rising air temperatures (Isaak et al., 2015). In systems with reliably cold channel

86   water in summer, which can also exist at low elevations when heavily influenced by discharging

87   groundwater, salmonid fish may directly use groundwater seepage zones for spawning rather

88   than thermal refuge.

89   Brook trout (*Salvelinus fontinalis*) are a species of char that are native to eastern North

90   America, from Georgia to Quebec (MacCrimmon and Campbell, 1969). Populations have been

91   stressed by warming temperatures and reduced water quality, particularly in low-elevation areas

92   (Hudy et al., 2008). Stream network-scale tracking of fish has indicated brook trout directly

93   utilize stream confluence mixing zones and preferential groundwater discharge to survive warm

94   summer periods (Baird and Krueger, 2003; Petty et al., 2012; Snook et al., 2016). Additionally,

95   brook trout spawn in the fall, and eggs deposited in redds develop over the winter before

96   hatching in spring (Cunjak and Power, 1986). Oxygen use by the shallow buried embryos

97   increases over the period of development (Crisp, 1981), and therefore DO concentration is a

98   critical parameter of the pore waters in which the eggs are bathed. Several studies have

99   demonstrated the importance of hyporheic downwelling in increasing shallow oxygen

100 concentrations, including at salmonid redds, where deeper streambed pore water is generally

101 reduced in DO (e.g. Buffington and Tonina 2009; Cardenas et al. 2016; Harvey et al.,

102 2013). Fine sediments can reduce the efficacy of hyporheic DO exchange in spawn zones

103 (Obruca and Hauer, 2016), and are actively cleared by trout during the spawning process

104 (Montgomery et al., 1996).

105   The importance of hyporheic exchange to salmonid spawning may be limited in the

106 lowland streams that are expected to harbor native cold-water species in the 21st century: those

107   with strong groundwater influence. Groundwater upwelling reduces the penetration of hyporheic

108   flow from surface water (Cardenas and Wilson, 2006) and may shut down hyporheic flushing in

109   redds (Cardenas et al., 2016). Where hyporheic exchange does introduce oxygenated channel

110   water into the shallow streambed, the downward advection of heat associated with near-freezing

111   surface water in winter will also cool streambed sediments (Geist et al., 2002), potentially

112   impairing egg development. Coaster brook trout, a life-history variant of native brook trout

113   exhibiting potadromous migrations within the Great Lakes, have been shown to specifically

114   prefer groundwater discharge zones for building redds (Grinsven et al., 2012). The development

115   of trout in winter has been found to be positively correlated with warmer stream water

116   temperatures as influenced by groundwater seepage (French et al., 2016), and therefore spatially

117   discrete groundwater discharge zones with adequate DO may form preferred brook trout

118   spawning habitat (Curry et al., 1995).

119   Multiscale physical and biogeochemical factors influence temperature and DO

120   concentrations along groundwater flowpaths. In river valleys, discharge to surface water of

121   locally recharged groundwater is expected to emanate from more shallow, lateral flowpaths

122   controlled by local topography (Modica, 1999; Winter et al., 1998). Shallow groundwater

123   flowpaths, particularly those within approximately 5 m of the land surface, will be more sensitive

124   to annual air temperature patterns and longer term warming trends due to strong vertical

125   conductive heat exchanges (Kurylyk et al., 2015b). The distance of seeps from upgradient

126   groundwater recharge zones will also affect seepage temperature dynamics and associated

127   aquatic ecosystems due to future changes in surface and recharge temperature (Burns et al.,

128   2017). Therefore, working backwards from thermal anomalies into the landscape is critical to

129   understanding the thermal stability of current and future point-scale preferential brook trout

130   habitat (Briggs et al., 2018a). The complimentary methodology of geophysical remote sensing,

131   geochemical sampling, and vertical bed temperature time series can indicate the physical and

132   chemical properties of groundwater flowpaths that source preferential discharge zones utilized

133   routinely by fish for spawning.

134   Coarse-grained mineral-dominated aquifers with little fine particulate organic matter and

135   low dissolved organic carbon supply tend to result in generally oxic groundwater conditions

136   (Back et al., 1993). The sandy surficial aquifer of Cape Cod, where our investigation took place,

137   is a classic example of a mineral soil-dominated flow system (Frimpter and Gay, 1979). Flow of

138   groundwater through near-stream organic deposits, however, can result in inverted redox

139   gradients toward the upwelling interface, such that groundwater discharged to surface water is

140   reduced in DO (Seitzinger et al., 2006). In sandy glacial terrain with superimposed peatland

141   deposits, the specific flow patterns of groundwater to surface water in relation to buried peat will

142   influence groundwater discharge biogeochemistry. Krause et al. (2013) found that streambed

143   groundwater seepage was strongly reduced in DO in zones with peat deposits, likely due to an

144   increase in both near-stream residence time and localized source of dissolved organic carbon.

145   Interdisciplinary collaborations between physical and biological scientists are useful to

146   better understand how cold-water species utilize groundwater discharge-influenced stream

147   habitat, and the larger landscape-scale controls on discharge characteristics. While previous

148   hydrogeological research in the coastal stream used for this study had focused on locating and

149   quantifying discrete groundwater discharge (e.g. "cold anomalies", Hare et al., 2015; Rosenberry

150   et al., 2016), here we endeavor to understand the hydraulic and biogeochemical controls on

151   seepage zone distribution utilized directly by native brook trout. In this groundwater-dominated

152   stream (e.g. likely climate refugia), brook trout do not need to occupy discrete inflows for

153   summer thermal refugia, but do favor certain upwelling zones for fall spawning. We compare

154   over a decade of visual survey and electronic fish passive integrated transponder (PIT)-tag

155   dropout data regarding repeat brook trout spawning locations to a comprehensive physical and

156   chemical characterization of groundwater seepage zones across 2-km of stream to:

157   1. Identify repeat brook trout spawning locations, and determine if they are directly

158   associated with the preferential discharge of groundwater through interface sediments.

159   2. Develop a hydrogeochemical characterization of trout-preferred groundwater discharge

160   zones that can aid in their identification in other less-studied systems and potential

161   inclusion in stream habitat restoration efforts.

162   **Site Description and Previous Hydrogeologic Characterization**

163   Cape Cod is a peninsula in southeastern coastal Massachusetts, USA, composed

164   primarily of highly permeable unconsolidated glacial moraine and outwash deposits. The largest

165   of the Cape Cod sole-source aquifers occupies a western (landward) section of the peninsula

166   (LeBlanc et al., 1986), and is incised by several linear valleys that drain groundwater south to the

167   Atlantic Ocean via baseflow-dominated streams (Figure 2a). Strong groundwater discharge to

168   one such stream, the Quashnet River, supports a relatively stable flow regime that has averaged

169   0.49 +/- 0.15 (SD) $m^3 s^{-1}$ from 1986-2015 (Rosenberry et al., 2016). The lower Quashnet River

170   emerges from a narrow sand and gravel valley to a broader area with well-defined lateral

171   floodplains. Historical cranberry farming practices, abandoned in the 1950s, have modified the

172   stream corridor (Barlow and Hess, 1993). Primary modifications included straightening of the

173   main channel (reducing natural sinuosity), installation of flood-control structures, incision of

174   shallow groundwater drainage ditches in the lateral peatland floodplain, and widespread

175 application of sand to the floodplain surface. The current bank-full width of the main channel

176 averages approximately 4 m.

177 The Quashnet River has long been recognized as critical habitat for a naturally reproducing

178 population of native sea-run brook trout (Mullan, 1958) with a genetically distinct population

179 (Annett et al., 2012). Efforts to restore trout habitat by the group *Trout Unlimited* and others

180 have been ongoing for over 40 yr (Barlow and Hess, 1993). These efforts include the removal of

181 flood-control structures and planting of trees along the main channel, and addition of wood

182 structures to stabilize banks and provide cover from airborne predators. Further, the

183 Commonwealth of Massachusetts purchased 12.5 hectares in 1956 and an additional 146

184 hectares along the lower Quashnet River in 1987 and 1988 to protect the area from development.

185 The Massachusetts Division of Fisheries and Wildlife has been monitoring trout populations

186 since 1988 and movement since 2007.

187 Groundwater influence on stream temperature is pronounced, particularly over the 2-km

188 reach above the USGS gage, below which stream stage is tidally affected. Ambient regional

189 groundwater temperature is approximately 11 °C (Briggs et al., 2014), and strong conductive and

190 advective exchange with the proximal aquifer maintains surface water temperature well below

191 the lethal threshold for brook trout (maximum weekly average temperature >23.3 °C, Wehrly *et*

192 *al.* 2007). Therefore point-scale thermal refugia are not a current concern in this system, as the

193 stream supports system-scale cold-water habitat that is likely to persist into the future and serve

194 as warming "climate refugia" (Briggs et al., 2018a). In winter, seepage zones can be located as

195 relatively warm anomalies increasing and buffering surface water temperatures from ambient

196 atmospheric influence.

197 Previous work has measured relatively large net gains in streamflow over the lower Quashnet

198   River (Barlow and Hess, 1993; Rosenberry et al., 2016), attributed to groundwater discharge

199   through direct streambed seepage and harvesting of groundwater from the floodplain platform

200   via relic agricultural drainage ditches. Deployments of fiber-optic temperature sensing (FO-DTS)

201   cables along the thalweg streambed interface indicate the greatest density of focused seepage

202   zones occurs along the broader valley area approximately 1 km upstream of the USGS gage

203   number 011058837; this zone coincides with the largest gains in net streamflow (Hare et al.,

204   2015). Based on the streambed interface temperature data presented by Rosenberry et al. (2016),

205   Figure 1 shows how temperature-sensitive fiber optic cables have been used to pinpoint possible

206   groundwater discharge zones based on anomalously cold mean temperature and/or reduced

207   thermal variance. Focused evaluation of FO-DTS anomalies with physical seepage meters and

208   vertical temperature profilers confirmed localized, meter-scale seepage zonation along the

209   streambed where discrete colder zones indicated through heat tracing showed approximately 5

210   times the groundwater discharge rate of adjacent sandy bed locations only meters away

211   (Rosenberry et al., 2016). Active heating of wrapped FO-DTS cables deployed vertically within

212   an open valley streambed seepage zone indicated true vertical flow to at least 0.6 m into the bed

213   sediments (Briggs et al., 2016), an expected characteristic of more regional groundwater

214   discharge (Winter et al., 1998), rather than that driven by valley topography local to the river.

215   Hyporheic exchange in the lower Quashnet River system is superimposed on the general upward

216   hydraulic gradient to the stream, and therefore reduced to a thin, shallow hyporheic exchange

217   zone (e.g. < 0.1 m depth) along the thalweg by these competing pressures (Briggs et al., 2014),

218   as has been simulated for similar stream systems (e.g. Cardenas and Wilson 2006).

219   **Methods**

220   A combination of fish tagging and visual spawning observations, heat tracing,

221   geophysical surveys, and focused pore-water sampling was used to investigate the interplay

222   between the locations of preferential brook trout spawning and the local hydrogeology. For

223   consistency between varied methods and years of data collection, all sample locations are

224   spatially referenced as downstream channel distance from the fish ladder river crossing at the

225   upper end of the study reach (Figure 2).

226   *Observations regarding repeat spawning locations*

227   Observations regarding discrete repeat brook trout spawning locations were made

228   opportunistically as part of an ongoing PIT tagging study of the native reproducing population of

229   the Quashnet River. Large-scale trout movements are continuously monitored in the lower

230   Quashnet River at 3 stationary fish counting sites (Figure 2a). However the spatial resolution of

231   these counting sites, separated by hundreds of meters, is not adequate to study how brook trout

232   utilize specific decimeter- to meter-scale groundwater discharge zones. For this finer scale

233   characterization, dropped fish tags have also been located through roving surveys using a

234   handheld portable PIT antenna (Biomark, Inc.) conducted in spring and fall since 2007. The

235   dropout of PIT tags from the fish body is a process that is more likely to happen during spawning

236   behavior in salmonids (Meyer et al 2011), so dropped tags were located electronically and

237   spatially mapped to reveal discrete zones of repeat spawning. Although these roving surveys do

238   not yield the temporal continuity of the instream counting gates, clustering of dropped tags can

239   be mapped at the sub-meter scale, presumably directly at trout redds. In addition, spawning

240   brook trout were located visually during annual fall data collection events by Massachusetts Fish

241   and Wildlife Staff, with redd development behavior captured within one seepage feature by

242   underwater video in 2015 using a GoPro Hero camera (San Mateo, CA). We refer to the 3 most

243   prominent sites of brook trout spawning within the study reach as Spawn 1 (113 m), Spawn 2

244   (146 m), and Spawn 3 (2062 m), from upstream to downstream, respectively (Figure 2).

245   *Spatial mapping of preferential groundwater discharges*

246   To augment existing streambed interface thermal surveys for preferential groundwater

247   discharge (e.g. Rosenberry et al., 2016; Figure 1) and the bank-dependence of discharge location,

248   ruggedized fiber-optic cables suitable for stream use were deployed in the river along the base of

249   each bank from 1700 to 2160 m on 10 June through 12 June 2016 (Figure 2a). Two separate

250   cables weighted with stainless steel armoring were installed directly along the foot of each bank

251   on top of the streambed interface. Single-ended measurements made at the 1.01 m linear spatial

252   sampling scale were integrated over 5-min intervals on each channel by an Oryx FO-DTS control

253   unit (Sensornet Ltd.). During the same period, data were also collected along a high-resolution

254   wrapped fiber-optic array for a dataset described in Kurylyk et al. (2017) but not shown here;

255   this experimental setup resulted in measurements for each channel of 4 instrument channels

256   recorded at 20-min intervals. Calibration for dynamic instrument drift was performed

257   automatically using an approximately 30-m length of cable for each channel submerged in a

258   continuously mixed ice-bath and monitored with an independent Oryx T-100 thermistor.

259   *Quantification of vertical groundwater discharge rates*

260   Once preferential discharge locations are located along the streambed with FO-DTS,

261   actual vertical discharge rates can be assessed with a variety of methodologies (Kalbus et al.,

262   2006). Temporal patterns in groundwater discharge flux rate can indicate source flowpath

263   hydrodynamics, and be derived from bed temperature time series using vertical temperature

264   signal transport characteristics, as reviewed by Rau et al., (2013). Custom "1DTempProfilers"

265   designed specifically for the quantification of groundwater discharge (Briggs et al., 2014) were

266   used to monitor streambed temperature over time along a shallow vertical profile. Profilers were

267   deployed within a subset of the thermal anomalies previously identified with FO-DTS. The

268   profiler deployment locations were chosen to represent a range of preferential groundwater

269   discharge rates/characteristics based on the on the observed FO-DTS temperature anomalies, e.g.

270   anomalies of varied mean temperature and buffering effect (Figure 1). These preferential

271   groundwater discharges were located: 330, 880, 1045, 1070, 1410, 1470, and 2060 m

272   approximate downstream distance from the fish ladder crossing. These groundwater discharge

273   locations are referred to with the prefix "GW" followed by the meter mark for the remainder of

274   the manuscript, such that major streambed seep 330 m downstream of the fish ladder is referred

275   to as "GW330". Data were collected at various locations from 11 June to 13 July 2014; 21

276   August to 13 September 2015; and 5 June to 9 July 2016. These deployments included

277   installation of 1DTempProfilers at the nearbank and channel sides of observed repeat spawning

278   zones.

279   Individual thermal data loggers (iButton Thermochron DS1922L, Maxim Integrated)

280   were waterproofed with silicone caulking and inserted horizontally into short slotted-steel pipes

281   (0.025 m diameter). The shallow thermal profilers were driven vertically into the streambed so

282   that sensors were positioned at some combination of 0.01, 0.04, 0.07, and 0.11 m depths. Data

283   were collected at temporal intervals of 0.5 hr in 2014, 2015, and 1 hr in 2016. Rosenberry et al.

284   (2016a) found that when a subset of the 2014 streambed temperature data presented here were

285   analyzed using the diurnal signal amplitude attenuation models employed by VFLUX2 (Irvine et

286   al., 2015), a near 1:1 relation was found in comparison to physical seepage meter measurements

287   of groundwater discharge ranging from 0.5 to 3 md^{-1}. A similar diurnal signal-based in-situ

288   streambed thermal parameter estimation is used here.

289 *Streambed groundwater discharge and spawning zone pore water characterization*

290   Subsurface water samples were collected for chemical analysis at 7 major open valley

291 seepage locations and 3 repeat spawn locations. Geochemical data collection occurred in 2014

292 and 2016 along with the 1DTempProfiler deployments, while stable water isotope data were

293 collection in August 2017. For geochemical sampling, 0.0095 m (nominal) stainless steel

294 drivepoints were inserted to depths of 0.3, 0.6, and/or 0.9 m and Masterflex Norprene tubing was

295 attached to the drivepoint. A peristaltic pump was used to extract pore water samples until free of

296 obvious turbidity (typically requiring 3 min of pumping) after which the pumping rate was

297 slowed and, the groundwater samples were collected by pumping into 60-mL HDPE syringe

298 barrels. First an unfiltered sample for specific conductivity was pushed from the syringe into a

299 30-mL HDPE Nalgene sample bottle. Second, a filtered sample for anion analysis was collected

300 after attaching a 0.2-µm pore size (25-mm diameter) Pall polyethersulfone filter to the syringe.

301 Lastly, the pumping rate was slowed again and an overflow cup was attached to the norprene

302 sample tubing and held upright until overflowing, at which point DO was measured by a field

303 colorimetric test using the manufacturer's evacuated reagent vials (Chemetrics V-2000). DO

304 concentrations were read twice and the test repeated using an alternative vial kit if results were

305 near the concentration range limit or out of range. The collected samples were kept cool and out

306 of the light and analyzed for Cl^- upon return to the laboratory using standard ion

307 chromatographic techniques.

308   In addition to the drivepoint samples, pore water samples were also collected in June

309 2016 from shallow depths 0.015, 0.04, 0.08 and 0.15 m below the streambed surface at locations

310 GW1045 and Spawn 1, 2, 3 using MINIPOINT samplers (e.g. Harvey and Fuller 1998). Water

311 was pumped simultaneously from all depths using a multi-head pump that withdrew small-

312   volume samples (15 mL) at low flow rates (1.5 mL min^{-1}) to minimize disturbance of natural

313   subsurface fluxes and chemical gradients. Pumped lines terminated at press-on luer fittings that

314   were pushed onto 0.2-µm pore size (25-mm diameter) Pall polyethersulfone filters. Samples for

315   specific conductivity were collected whereas filtered samples were collected for anions in

316   prelabeled 20-mL LDPE plastic scintillation vials with Polyseal^{TM} caps. Sample lines were then

317   attached to overflow cups and dissolved oxygen concentrations were measured as described

318   above.

319   During a follow-up field effort in August, 2017 streambed pore water samples were

320   collected at the Spawn sites and at GW1045, GW1140 (approximately 70 m downstream of

321   GW1070), and GW1470. Additionally, two large hillslope springs were identified along the edge

322   of the riparian zone, upstream of Spawn 1, using a handheld thermal infrared camera (FLIR

323   T640, FLIR Systems, Inc.). These exposed springs were sampled to identify a localized hillslope

324   groundwater signature that would not be impacted by valley-floor peat deposits. Samples were

325   drawn from push-point piezometers installed from 0.2-0.44 m below the sediment interface, with

326   deeper samples collected in the hillslope springs to avoid surface organic material. Pore water

327   was evaluated for specific conductivity (SpC), DO, and stable water isotopes. Isotope samples

328   were analyzed by the U.S. Geological Survey Stable Isotope Laboratory using dual-inlet isotope-

329   ratio mass spectrometry. A substantial fraction of regional Cape Cod shallow groundwater

330   exchanges with the numerous groundwater flow through lakes as it discharges to the coast

331   (Walter and Masterson, 2002). It is therefore assumed that the regional Cape Cod groundwater

332   isotopic signature is likely to indicate evaporative processes (Leblanc et al., 2008), offering a

333   contrasting signal from locally recharged hillslope groundwaters (no substantial evaporation).

334   Local deuterium excess of contemporary waters can indicate groundwater that has been

335   influenced by evaporation in lakes, and is therefore in disequilibrium with local meteoric waters.

336   Deuterium excess was determined here as: $d\text{-}xs=\delta^2 H - 8* \delta^{18}O$ (Dansgaard, 1964).

337   As mentioned previously, historic cranberry farming practices extensively modified the

338   Quashnet River valley including the incision of drainage ditches into the floodplain. Some

339   ditches extend from the valley wall to the main channel, whereas others are shorter or cut at

340   angles. In addition to characterization of pore water, 34 major drainage ditches (observed

341   flowing water) and a stream thalweg profile were spot checked for specific conductivity on 16

342   June 2014 using the SmarTroll probe (YSI). At a subset of these ditch locations, filtered grab

343   samples were collected and analyzed in the laboratory for Cl^- in a similar manner as for the mini

344   and drivepoint samples described above. In June 2016, the dataset was augmented for 5 ditch

345   confluence locations upstream of Spawn 1.

346   *Visualizing streambed sediment geologic structure*

347   Ground penetrating radar (GPR) has been successfully applied to several surface

348   water/groundwater exchange studies to characterize underlying peat and sandy deposits (e.g.

349   Lowry et al., 2009; Comas et al., 2011) due to strong expected differences in matrix porosity

350   (water content), which can exceed 70% in peat (Rezanezhad et al., 2016). An upstream to

351   downstream GPR profile was collected on 7 July 2016 using a MALA HDR GX160 shielded

352   antenna (MALA GPR, Sweden) hand-towed down the stream center channel with a small

353   inflatable watercraft. The locations of major seep and spawning sites were specifically marked

354   on the digital GPR record during data collection. The GPR data were processed using Reflexw

355   software (Sandmeier, Germany) to convert reflection time to interface depth.

356   **Results**

357   The hydrogeochemical characterization of observed, repeat trout spawning zones and

358   other major streambed groundwater discharge zones are contrasted below.

359   *Observations regarding repeat spawning locations*

360   Out of the dozens of preferential groundwater discharge zones geolocated along the

361   Quashnet River in this and previous work (e.g. Figure 1), brook trout appear to consistently

362   utilize only three discrete streambed locations for repeat spawning activity. These locations

363   coincide with steep cut banks where the river channel approaches the sand and gravel valley wall

364   (Figure 2b,c). Specifically, trout were found to occupy small "scalloped" alcove bank features

365   (Figure 3a) that may be formed by groundwater sapping and subsequent slumping of sandy bank

366   materials. In winter 2016, fresh slumping and direct seepage from the newly exposed sand wall

367   was observed at Spawn 3 (Figure 3c); a larger slump event had filled approximately 1/3 of the

368   scalloped alcove at Spawn 2 by June 2016. Brook trout were observed clustered along the inner

369   bank area at the Spawn 1 location in fall 2015 (Figure 3d), and this spawning behavior was

370   captured using underwater video (Supplemental Video S1).

371   Dropout PIT tags have been found repeatedly in each of the 3 preferential spawn zones.

372   Seven dropout PIT tags were located in the Spawn 3 zone in March 2017, by far the most

373   dropped tags found in any one location since the tracking program began in 2007. The only other

374   obvious scalloped bank features along the 2 km study reach are located at GW1045 (Figure 3b).

375   Compared to the trout spawning zone alcoves along the valley wall cutbanks (e.g. Figure 3a),

376   this open valley seepage alcove was overgrown with watercress and thick (tens of centimeters)

377   loose deposits of organic material.

378   *Spatial mapping of preferential groundwater discharges*

379   As shown in Figure 1, previously collected FO-DTS data were used to guide data

380   collection at a subset of representative preferential streambed groundwater discharges.

381   Additionally, paired FO-DTS cables were deployed at the base of both stream banks through a

382   lower reach section in 2016 (Figure 2c), revealing differing thermal anomaly patterns (Figure 4;

383   Briggs et al., 2018b). The cable along the downstream-right bank captures a large, 8-m-long

384   cooler zone at Spawn 3 (Figure 4b), and this seepage signature is spatially reduced but visible

385   along the opposing bank (Figure 4a). Other thermal anomalies observed along one bank show

386   little or no signature along the other. Air temperature dropped noticeably over the final 1.5 d of

387   deployment, and smaller cool anomalies that appeared on warm days are no longer captured by

388   the streambed FO-DTS deployment, but the Spawn 3 signature is still visible along both cables.

389   *Quantification of vertical groundwater discharge rates*
390   Ambient streambed temperature signal data can be used to measure streambed thermal

391   conduction parameters (Luce et al., 2013), which is particularly important when applying heat-

392   based methods to quantify upward vertical fluid flux (Rosenberry et al., 2016), compared to

393   downward fluid flux models that generally show less sensitivity to streambed thermal

394   parameters. Diurnal signal-based thermal diffusivity measurements derived from a pair of

395   1DTempProfilers inserted in sandy channel sediments for a month in 2014 have the same

396   geometric mean value of 0.11 m^2d^{-1} (Briggs et al., 2018b), and this value is used here to model

397   vertical groundwater discharge for all locations and data collection periods (Briggs et al., 2018b)

398   . Sub-daily groundwater discharge fluxes evaluated over similar spring/early summer time

399   periods in 2014 and 2016 show relatively stable patterns at open valley seepage zones, generally

400   <1 md^{-1} (Figure 6). At Spawn 1 and 3 seepage is stronger (2 to 3.5 md^{-1}) and more variable than

401   at open valley zones. The Darcy-based horizontal seepage estimate through the Spawn 3 bank,

402   made using the bank piezometer, is 2.3 md^{-1}, which is similar to the temperature-based seepage

403   rates at the Spawn 3 interface (Figure 6), and indicates lateral discharge through the cut bank

404   wall from a more localized groundwater flowpath. The Spawn 2 zone shows a reduced and more

405   stable discharge rate during summer 2016, and is likely impacted by a large bank slump into this

406   zone that occurred during the winter of 2016, partially filling the alcove. Seepage patterns

407   collected at Spawn 1 and 2 in late-summer 2015 show greater temporal stability, even though the

408   stream stage at the downstream USGS gage showed substantial variation. Discharge rates along

409   the inner bank wall of the scalloped bank spawn zones were consistently higher than at bed areas

410   located just a few meters away toward the channel.

411   *Streambed groundwater discharge and spawning zone pore water characterization*

412   Based on previous characterization, the Cape Cod sand and gravel aquifer generally has

413   high DO concentrations (9 - 11 mg/L), relatively dilute specific conductance (SpC, 62 µS/cm),

414   and dilute chloride concentrations (Cl$^-$, 9.3 mg/L) at depths ranging between 12 and 20 m

415   (Savoie et al., 2012). The groundwater that discharges to the Quashnet River, however, is often

416   strongly variable in all three of these parameters (Harvey et al., 2018). In June 2014, drivepoint

417   data were primarily collected in open valley seepage zones identified with FO-DTS (Figure 1);

418   these locations are suboxic to anoxic at 0.3 and 0.6 m streambed depths (Table 1). Highest

419   streambed seepage DO is found at GW330 in the tighter upstream valley section (4.6 mg/L at

420   both depths) and Spawn 3, where DO is 9.0 and 7.6 mg/L at 0.3 m and 0.6 m depths,

421   respectively (Table 1). SpC is also variable, but lowest and similar to the regional signal at

422   GW330 and Spawn 3. Note, SpC and Cl$^-$ are used here to indicate aquifer flowpath

423   hydrogeochemical properties, and not suitable spawn habitat based on chemical concentration, as

424   their range is well within general brook trout tolerances.

425   Drivepoint data collected at the 0.3 m depth in June 2016, primarily around spawn zones,

426   generally show high DO and relatively low SpC at the interior of Spawn Zones 1 and 3 near the

427   cut bank (Table 1). Data collected a few meters toward the main channel from these near-bank

428   spawn locations are reduced in DO with increased SpC. The Spawn 2 data were collected at the

429   toe of the recent large sediment slump that had partially filled the alcove, and DO data are

430   suboxic at 0.3 m (3.9 mg/L) but more oxygen enriched at 0.9 m depth (7.2 mg/L) indicating the

431   potential for shallow streambed respiration that removes oxygen from discharging groundwater

432   (assuming vertical flow) in the slumped material. In contrast to the spawn zones, major open

433   valley seepage location GW1045 is nearly anoxic at all depths with SpC similar to the 2014

434   stream water profile grab samples (n=8, 101.4 +/- 1.7 µS/cm). Little difference was observed

435   between near-bank and channel positions at GW1045 (both are suboxic) even though a large

436   scalloped seepage bank feature was observed (Figure 3b).

437   The drainage-ditch grab samples generally show Cl$^-$ concentrations that are lower than

438   the average 2014 channel grab samples (n=10, 19 +/- 0.4 mg/L), though the 2 most upstream

439   ditches are similar to stream water, and 2 open valley ditches are appreciably higher in Cl$^-$

440   (Figure 7a). Spawn Zones 1, 2, and 3 approximate the lowest Cl$^-$ concentrations observed in

441   drainage ditches, and Spawn 3 has a similar concentration to the adjacent 2016 streambank

442   piezometer in both the 2014 and 2016 data. An analogous pattern is shown in the more

443   widespread SpC data, with many drainage ditches and all spawn zones having concentrations

444   around 60 µS/cm, but several ditches cluster around the stream water average or higher,

445   particularly in the open valley area.

446   The shallow, discrete interval shallow pore-water samples collected with the

447   MINIPOINT system show that streambed SpC is appreciably lower than stream water, even at

448   the 0.02 m depth, at all near-bank spawn zones (Figure 8a). Conversely, the shallow channel

449   sediments at Spawn 1 and open valley seepage GW1045 approximate the stream water value for

450   SpC. DO is high and stable along the shallow profiles (to 0.14 m) at the interior of Spawn Zones

451   1 and 3, but suboxic at the Spawn 1 channel sample and Spawn 2 zones, and essentially anoxic

452   along the bank at GW1045 . Center channel pore water samples at GW1045 show moderate

453   oxygen enrichment at 0.02 m (4.6 mg/L), which may result from hyporheic mixing, as deeper

454   intervals along the same profile are nearly anoxic.

455   Underwater video collected here in the fall of 2015 indicates Quashnet River brook trout

456   clustered tightly around an approximate 1-m^2 bed area in Spawn 1 (Figure 3d, Video S1),

457   directly at the base of the sandy cut bank. During the June 2016 collection of pore-water data,

458   drivepoints were installed precisely in this area. Chemical analysis of 0.3 m depth pore water

459   shows a strong gradient from the near-bank Spawn 1 zone to the outer alcove area, with specific

460   conductance rising dramatically (70.6 to 143.9 µS/cm) and DO falling (7.28 to 4.41 mg/L)

461   (Table 1). Spawn 3 shows a similar pattern from near-bank toward main channel (60.4 to 82.1

462   µS/cm SpC; 9.11 to 1.76 mg/L DO), and Spawn 2, although complicated by the large slump

463   during the previous winter, shows an increase in SpC from 70.6 to 139.3 µS/cm from the inner to

464   outer alcove. Conversely, pore water collected at 0.3, 0.6, and 0.9 m depths in the open valley

465   seepage alcove at GW1045 (pictured in Figure 3b) are functionally anoxic with elevated SpC

466   compared to inner spawn zones, and little gradient from bank to channel.

467   Pore water data collected in August 2017 indicate that all three Spawn sites are similar to

468   emergent hillslope springs, characterized by relatively high DO and low SpC compared to major

469   open valley streambed seepage zones that are anoxic with higher SpC (Table 2). Additionally,

470   the stable isotopic signatures of the hillslope and Spawn zones are similar, but contrasted by the

471 lower deuterium excess metric determined for the open valley seepages. This indicates that

472 groundwater discharging through the streambed away from the hillslope shows the evaporative

473 signature of groundwater flow through lakes, and can therefore be considered regional discharge,

474 compared to locally recharged hillslope groundwaters apparently favored be trout for spawning..

475 *Visualizing streambed sediment geologic structure*
476   Radar data were collected over most of the study reach length depicted in Figure 2a, and

477 although spatial reference data were not collected for each sample point due to integrated global

478 positioning system failure, Spawn and groundwater discharge zones of interest were precisely

479 marked in the record (Figure 5). The GPR data collected along the thalweg adjacent to Spawn 1

480 and 2 indicate a contiguous thin layer of material underlies the sandy streambed that may be peat

481 deposited over deeper sands and gravels (Figure 5a). The GPR profile through open valley

482 groundwater discharge locations GW1045 and GW1070 show the strongest radar signal

483 reflectors of anywhere along the open valley section (Figure 5b). These discontinuous geologic

484 structures are interpreted as layered sand, gravel, interspersed with thicker peat deposits.

485 Otherwise, discontinuous reflections indicative of sediment type-interfaces of variable depth are

486 observed near downstream open valley seepage zones where strongly attenuated GPR signals

487 indicate thick lenses of buried peat with high water content (Figure 5b,c).

488 **Discussion**

489   Heat tracing reconnaissance technologies, such as FO-DTS and thermal infrared, offer an

490 efficient means to comprehensively characterize a subset of preferential groundwater discharge

491 points at the reach to watershed scale (Briggs and Hare, 2018). Using the groundwater-fed

492 Quashnet River as an example, Rosenberry et al. (2016) showed that cold streambed interface

493 anomalies in summer indeed corresponded to discrete zones of particularly high groundwater

494   discharge through streambed sediments. This spatial characterization of discharge points alone is

495   not sufficient to characterize the physical and chemical drivers of niche critical cold-water

496   habitat, but can efficiently guide additional data collection, as was done here. Compared to more

497   randomly distributed streambed field parameter surveys, or larger spatial scale evaluations of net

498   groundwater discharge made with differential gaging, comprehensive spatial mapping of

499   groundwater discharges is a great advance in the context of understanding groundwater

500   dependent ecosystems. However, in fast flowing streams, FO-DTS cable placement on the

501   streambed will likely impact which specific groundwater discharge zones are captured with FO-

502   DTS, as shown here by applying cables along opposite banks through the Spawn 3 area (Figure

503   4). The largest seepage zones may have a spatial footprint that encompasses the streambed area

504   from bank to bank (e.g., the Spawn 3 cold anomaly), but a subset of more discrete seepage zones

505   are bound to be missed with a single linear cable deployment. We did not capture Spawn Zones 1

506   and 2 in early FO-DTS field efforts (Figure 1), but fish tracking indicated their importance to

507   trout spawning behavior. Therefore, in studies of niche stream habitat as influenced by

508   preferential groundwater discharge, a combination of heat tracing and biological observation

509   may be needed to both identify major discharge points and discern which points are directly used

510   by the biota of interest (e.g. brook trout).

511   In a study of the regional Cape Cod aquifer condition, Frimpter and Gay (1979) state that

512   groundwater is typically near DO saturation, except downgradient of peat or river bottom

513   sediments, where consumption of DO allows the mobilization of natural iron and manganese.

514   Visible observations along the open valley section, in addition to streambed sediment coring

515   (Briggs et al. 2014), revealed widespread coating of shallow streambed sediment grains with

516   metal oxides, consistent with the conceptual model of organic material influence on near-surface

517   groundwater (Figure 9). Aquifer recharge passing through upgradient groundwater flow-through

518   kettle lakes (e.g. Stoliker *et al.* 2016) may also serve to decrease the DO content of regional

519   flowpaths that discharge vertically through the bed of the Quashnet River, although we

520   hypothesize that localized peat deposits may be the primary control on both seepage zone

521   distribution and chemistry.

522   Out of the dozens of preferential groundwater discharge zones located along the lower

523   Quashnet with heat tracing, most were suboxic to anoxic (Table 1). Brook trout consistently

524   prefer three areas for fall spawning, all along meander bend cut banks into the sand and gravel

525   valley wall. Zones of locally enhanced seepage, likely controlled by subtle differences in

526   sediment hydraulic conductivity, can lead to groundwater sapping of fines, reduction in bank

527   stability, and consequent slumping of bank material into the river; this process was observed in

528   real-time at the Spawn 3 meander in February 2016 (Figure 3c). Slumping effectively forms

529   *seepage-driven* alcoves outside of the main flow and more suitable for redd placement, along

530   with a more favorable coarse sand and gravel substrate (Bowerman et al., 2014; Hausle and

531   Coble, 1976; Raleigh, 1982).

532   In other systems, trout have been observed to occupy microhabitat around and within

533   groundwater discharge zones, even segregating by fish size and desirable temperature range

534   (e.g., Figure 2.4.1.2 in Torgersen et al. 2012). Here, real-time observation and visual imagery

535   show trout clustering tightly against the bank in Spawn 3 (Figure 3d, Video S1) where pore

536   water was found to be more oxygen rich and lower in SpC. Month-long time series of vertical

537   groundwater discharge rates are reduced considerably from near-bank to near-channel at all

538   spawning zones (Figure 6), indicating in part a reduction in streambed hydraulic conductivity as

539   influenced by peat deposits under the main channel as observed in GPR data (Figure 5). The

540   combined evidence of higher near-bank vertical groundwater flux rates and DO, combined with

541   lower SpC, indicates limited interaction between shallow groundwater flowpaths and peat

542   against the meander bend cut banks. It appears that even short travel distances through organic

543   deposits toward the center channel at Spawn 1 and 2 may be sufficient to increase total dissolved

544   solids and deplete DO, as observed in other systems (e.g. Levy et al., 2016), and render

545   upwelling zones undesirable for redd construction. Therefore, near-surface channel sediments

546   may need to be specifically characterized in preferential groundwater discharge zones, as net

547   chemical reactivity over the last ~1 m of transport may dominate that along km of upgraient

548   groundwater flow through mineral soils.

549   Only where seepage was observed to emanate directly from the valley wall sands and

550   gravels, such as the newly exposed slump in Figure 3C, may groundwater discharge reliably

551   support overwinter trout egg development. These features are apparently similar to the numerous

552   cold-water alcove patches observed in another stream system by Ebersole et al. (2003). In that

553   study of preferential salmonid habitat, alcoves were often located where streams converged on

554   valley walls and were the most abundant type of discrete cold-water habitat type identified.

555   Conversely, valley wall alcoves were the least-common type of seep morphology observed along

556   the Quashnet River. It is likely that the artificial reduction in channel sinuosity along the

557   Quashnet River by farming practices has reduced the number of natural higher-quality spawning

558   locations.

559   Other bank alcove features with strong groundwater discharge found along the open

560   valley section (Figure 3b) were highly influenced by organic material deposition and did not

561   apparently support spawning habitat. Our research indicates that in lowland systems with

562   organic-rich floodplain sediments valley wall alcoves alone create favored brook trout spawning

563   habitat via local mineral soil-dominated groundwater discharge flowpaths as shown in

564   conceptual Figure 9. This finding might help inform future ecologically based stream restoration

565   practices in using the natural landscape to predict desirable preferential groundwater discharge

566   points, as was recently done by Hare et al., (2017) to inform the engineering of a large-scale

567   cranberry bog restoration.

568   The pore-water SpC, Cl-, and DO data alone do not definitively show that seepage at the

569   cut bank spawn sites is derived from more localized groundwater recharge, as opposed to

570   regional groundwater that is unadulterated by buried peat lenses. However, the hydrodynamic

571   data derived from long-term vertical temperature profiling in seepage zones does offer additional

572   insight. In general, groundwater discharge rates are more variable at cut bank spawn zones than

573   in the open valley streambed zones (Figure 6), and this variability may be tied to shorter-term

574   changes in local river stage and/or water table depth, impacting the local hydraulic gradient. The

575   relatively stable patterns of open valley groundwater discharge may be controlled by the regional

576   gradient where the flowpath-length term dominates the Darcy relation, and is therefore relatively

577   insensitive to local changes in river stage and water table fluctuations. Further, the stable water

578   isotope data display evaporative signatures at the open valley streambed discharge sites,

579   indicating regional groundwater that has passed through one or more upgradient flow-through

580   lakes (Table 2). In contrast, the Spawn sites all show isotope signals that fall along the local

581   meteoric water line, and therefore likely represent recharge to the hillslopes more local to the

582   river. These localized groundwater flow systems would be expected to be less-influenced by

583   regional groundwater contamination, which is widespread in the regional Cape Cod aquifer

584   (Walter and Masterson, 2002).

585   Groundwater drainage-ditch data collected along the river corridor indicate low SpC/Cl-

586 conditions exist for the majority of ditches throughout the lower Quashnet River riparian areas

587 (Figure 7). The hillslope piezometer in sand and gravel at the down valley wall has a similar

588 chemical signature along with high DO. This similarity is further indication that low-SpC

589 groundwater discharges even to the lower portion of the river corridor, but is predominantly

590 modified chemically by travel through near-stream organics. The relic drainage ditches allow

591 discharging groundwater to effectively short circuit the valley floor peat deposits and remain

592 high in DO, similar to the natural valley wall springs and cut bank alcoves. Future restoration

593 strategies that seek to actively enhance groundwater discharge (e.g. Kurylyk et al., 2015a) may

594 consider capitalizing on this short circuit behavior, possibly by auguring through buried

595 streambed peat or movement of the stream channel toward the valley wall to create more

596 desirable brook trout aquatic habitat.

597 **Conclusions**

598   The three repeatedly utilized discrete spawning zone locations that have been identified

599 for over a decade of observation have coupled strongly discharging groundwater with high DO

600 concentration. A conceptual diagram of the hydrogeochemical setting of spawn zones vs other

601 non-favored streambed groundwater discharge locations is shown in Figure 9. Spawn zones are

602 located exclusively in side alcoves of the channel created by bank slumps along meanders where

603 the river cuts into steep hillslopes along the glacial sands and gravel valley wall. In the alcoves at

604 the base of the cut banks, hillslope groundwater with high DO concentration is discharged

605 through the streambed without appreciable loss of oxygen. Just a few meters away toward the

606 main channel, however, groundwater consistently discharges at lower rates, is reduced in DO,

607 and increased in SpC. The lowest oxygen concentrations in groundwater are associated with

608 water emerging from the streambed adjacent to wide riparian areas that flank the Quashnet in the

609   open valley section of the study reach, even though groundwater discharge rates were also

610   relatively high. In the open valley, where the stream is not near the valley walls, proximity to the

611   stream bank does not seem to control seepage chemistry, and GPR data indicated thick zones of

612   discontinuous streambed peat. In this and other groundwater-dominated streams that are

613   expected to serve as climate refugia for future native trout populations, hyporheic exchange will

614   be limited by strong upward hydraulic gradient. Therefore, preferential spawning habitat in such

615   lowland valley systems may be primarily supported by discrete zones of oxic groundwater

616   upwelling at the meter to sub-meter scale as has been indicated by previous work (e.g. Curry et

617   al., 1995).

618   In systems where all groundwater discharge is universally anoxic, preferential salmonid

619   spawning zonation may be controlled by points of downwelling hyporheic water where shallow

620   sediments remain high in DO (Buffington and Tonina, 2009; Cardenas et al., 2016). However,

621   these hyporheic areas will deliver cold surface water to shallow sediments during winter, which

622   may impair overwintering brook trout eggs (French et al., 2016). Here, and in many other coastal

623   systems, groundwater temperature is expected to range approximately 10-12 $^{\circ}$C, which is an

624   ideal range for brook trout egg development (Raleigh, 1982). Points of oxic groundwater

625   upwelling devoid of near-stream buried organics, combined with a recirculating side alcove and

626   favorable sand and gravel sediments, may provide ideal and unique groundwater seepage-

627   enabled preferential spawning habitat for native trout.

628   Stream surface or streambed interface heat tracing of groundwater discharge offers an

629   efficient means to locate discrete seepage zones, but offers only limited insight into source

630   groundwater flowpath hydraulics and geochemistry. A combined toolkit that also includes

631   spatially-informed (using heat tracing) geochemical and isotope sampling and geophysical

632 imaging can be used to trace groundwater flowpaths back into the source aquifer, and develop a

633 robust hydrogeochemical characterization. Additionally, as digital elevation models become

634 more refined and combined with infrared data derived from unmanned aerial systems, remote

635 identification of relatively small features such as the seepage alcoves described here should be

636 possible. Comprehensive and process-based characterization niche stream habitat can be used to

637 guide stream ecological restoration design that directly incorporates the local preferential

638 groundwater discharge template.

639 **Acknowledgements**

640   Comments from anonymous reviewers and U.S. Geological Survey (USGS) reviews by

641 Nathaniel Hitt and Paul Barlow are gratefully acknowledged. The U.S. Environmental Protection

642 Agency (USEPA) through its Office of Research and Development partially funded and

643 collaborated in the research described here under agreement number DW-14-92381701 to the

644 USGS. The USGS authors were supported by the following USGS entities: Office of

645 Groundwater, Water Availability and Use Science Program, National Water Quality Program,

646 and the Toxics Substances Hydrology Program. Field and laboratory assistance from Allison

647 Swartz, Jay Choi, Jenny Lewis, Yao Du, Danielle Hare, Courtney Scruggs, Rayna Mitzman,

648 David Rey, Geoff Delin, Eric White, MassWildlife Southeast District Staff, Jennifer Salas, and

649 volunteers from Trout Unlimited is greatly appreciated. The manuscript has been subjected to

650 Agency review and approved for publication. The views expressed in this article are those of the

651 authors and do not necessarily represent the views or policies of the USEPA. Any use of trade,

652 firm, or product names is for descriptive purposes only and does not imply endorsement by the

653 U.S. Government.

654

References

Annett, B., Gerlach, G., King, T. L. and Whiteley, A. R.: Conservation Genetics of Remnant Coastal Brook Trout Populations at the Southern Limit of Their Distribution: Population Structure and Effects of Stocking, Trans. Am. Fish. Soc., 141(5), 1399–1410, doi:10.1080/00028487.2012.694831, 2012.

Back, W., Baedecker, M. J. and Wood, W. W.: Scales in hydrogeology: a historical persective, in Regional Water Quality, pp. 11–128, Van Nostrand Reinhold, New York., 1993.

Baird, O. E. and Krueger, C. C.: Behavioral thermoregulation of brook and rainbow trout: comparison of summer habitat use in an Adirondack River, New York, Trans. Am. Fish. Soc., 132, 1194–1206, 2003.

Barlow, P. M. and Hess, K. M.: Simulated Hydrologic Responses of the Quashnet River Stream-Aquifer System to Proposed Ground-Water Withdrawals, Cape Cod, Massachusetts, U.S. Geol. Surv. Rep. 93-4064, 51, 1993.

Bowerman, T., Neilson, B. T. and Budy, P.: Effects of fine sediment, hyporheic flow, and spawning site characteristics on survival and development of bull trout embryos, Can. J. Fish. Aquat. Sci., 71, 1059–1071, 2014.

Briggs, M. A., Lautz, L. K., Buckley, S. F. and Lane, J. W.: Practical limitations on the use of diurnal temperature signals to quantify groundwater upwelling, J. Hydrol., 519, 1739–1751, doi:10.1016/j.jhydrol.2014.09.030, 2014.

Briggs, M. A., Buckley, S. F., Bagtzoglou, A. C., Werkema, D. and Lane, J. W.: Actively heated high-resolution fiber-optic distributed temperature sensing to quantify flow dynamics in zones of strong groundwater upwelling, Water Resources Research, 52, doi: 10.1002/2015WR018219, 2016.

Briggs, M. A., Johnson, Z. C., Snyder, C. D., Hitt, N. P., Kurylyk, B. L., Lautz, L., Irvine, D. J., Hurley, S. T. and Lane, J. W.: Inferring watershed hydraulics and cold-water habitat persistence using multi-year air and stream temperature signals, Sci. Total Environ., 636, 1117–1127, doi:10.1016/j.scitotenv.2018.04.344, 2018a.

Briggs, M. A., Scruggs, C. R., Hurley, S. T. and White, E. A.: Temperature and geophysical data collected along the Quashnet River, Mashpee/Falmouth MA: U.S. Geological Survey data release, doi:10.5066/F7PN93QF, 2018b.

Briggs, M. A. and Hare, D. K.: Explicit consideration of preferential groundwater discharges as surface water ecosystem control points, Hydrological Processes, 10.1002/hyp.13178, 2018.

Buffington, J. M. and Tonina, D.: A three-dimensional model for analyzing the effects of salmon redds on hyporheic exchange and egg pocket habitat A three-dimensional model for analyzing the effects of salmon redds on hyporheic exchange and egg pocket habitat, Can. J. Fish. Aquat.

690   Sci., 66, 2157–2173, doi:10.1139/F09-146, 2009.

691   Burns, E. R., Zhu, Y., Zhan, H., Manga, M., Williams, C. F., Ingebritsen, S. E. and Dunham, J.:
692   Thermal effect of climate change on groundwater-fed ecosystems, Water Resour. Res., 53,
693   3341–3351, doi:10.1002/2016WR020007, 2017.

694   Cardenas, M. B. and Wilson, J. L.: The influence of ambient groundwater discharge on exchange
695   zones induced by current-bedform interactions, J. Hydrol., 331(1–2), 103–109, 2006.

696   Cardenas, M. B., Ford, A. E., Kaufman, M. H., Kessler, A. J. and Cook, P. L. M.: Hyporheic
697   flow and dissolved oxygen distribution in fish nests: the effects of open channel velocity,
698   permeability patterns, and groundwater upwelling, J. Geophys. Res. Biogeosciences, 121, 3113–
699   3130, doi:10.1002/2016JG003381, 2016.

700   Comas, X., Slater, L. and Reeve, A. S.: Pool patterning in a northern peatland: Geophysical
701   evidence for the role of postglacial landforms, J. Hydrol., 399(3–4), 173–184,
702   doi:10.1016/j.jhydrol.2010.12.031, 2011.

703   Crisp: A desk study of the relationship between temperature and hatching time for the eggs of
704   five species of salmonid species, Freshw. Biol., 11(4), 361–368, doi:10.1111/j.1365-
705   2427.1981.tb01267.x, 1981.

706   Cunjak, R. A. and Power, G.: Seasonal changes in the physiology of brook trout, Salvelinus
707   fontinalis (Mitchill), in a sub-Arctic river system, J. Fish Biol., 29, 279–288, 1986.

708   Curry, R., Noakes, D. L. G. and Morgan, G. E.: Groundwater and the incubation and emergence
709   of brook trout (Salvelinus fontinalis), Can. J. Fish. Aquat. Sci., 52, 1741–1749, 1995.

710   Dansgaard, W.: Stable isotopes in precipitation, Tellus, 16(4), 436–468,
711   doi:10.3402/tellusa.v16i4.8993, 1964.

712   Dugdale, S. J.: A practitioner's guide to thermal infrared remote sensing of rivers and streams:
713   recent advances, precautions and considerations, WIREs Water, doi:10.1002/wat2.1135, 2016.

714   Dugdale, S. J., Bergeron, N. E. and St-Hilaire, A.: Spatial distribution of thermal refuges
715   analysed in relation to riverscape hydromorphology using airborne thermal infrared imagery,
716   Remote Sens. Environ., 160, 43–55, doi:10.1016/j.rse.2014.12.021, 2015.

717   Ebersole, J. L., Liss, W. J. and Frissell, C. A.: Cold water patches in warm streams:
718   physicochemical characteristics and the influence of shading, J. Am. Water Resour. Assoc.,
719   59860, 355–368, 2003.

720   French, W. E., Vondracek, B., Ferrington, L. C., Finlay, J. C. and Dieterman, D. J.: Brown trout
721   (Salmo trutta) growth and condition along a winter thermal gradient in temperate streams, Can. J.
722   Fish. Aquat. Sci., 9(June), 1–9, doi:10.1139/cjfas-2016-0005, 2016.

723   Frimpter, M. H. and Gay, F. B.: Chemical quality of ground water on Cape Cod, Massachusetts,
724   Water-Resources Investig. Rep. 79-65, 1979.

725   Geist, D. R., Hanrahan, T. P., Arntzen, E. V, Mcmichael, G. A., Murray, C. J. and Chien, Y.:

726 Physicochemical Characteristics of the Hyporheic Zone Affect Redd Site Selection by Chum
727 Salmon and Fall Chinook Salmon in the Columbia River, North Am. J. Fish. Manag., 22, 1077–
728 1085, 2002.

729 Grinsven, M. Van, Mayer, A. and Huckins, C.: Estimation of Streambed Groundwater Fluxes
730 Associated with Coaster Brook Trout Spawning Habitat, , 50(3), 432–441, doi:10.1111/j.1745-
731 6584.2011.00856.x, 2012.

732 Hare, D. K., Briggs, M. A., Rosenberry, D. O., Boutt, D. F. and Lane, J. W.: A comparison of
733 thermal infrared to fiber-optic distributed temperature sensing for evaluation of groundwater
734 discharge to surface water, J. Hydrol., 530, 153–166, doi:10.1016/j.jhydrol.2015.09.059, 2015.

735 Hare, D. K., Boutt, D. F., Clement, W. P., Hatch, C. E., Davenport, G. and Hackman, A.:
736 Hydrogeological controls on spatial patterns of groundwater discharge in peatlands, Hydrol.
737 Earth Syst. Sci., (21), 6031–6048, doi:10.5194/hess-2017-282, 2017.

738 Harvey, J. W. and Fuller, C. C.: Effect of enhanced manganese oxidation in the hyporheic zone
739 on basin-scale geochemical mass balance, , 34(4), 623–636, 1998.

740 Harvey, J. W., Briggs, M. A., Buskirk, B., Swartz, A., Lewis, J. and Du, Y.: Surface water and
741 groundwater water chemistry data collected along the Quashnet River, Mashpee/Falmouth, MA:
742 U.S. Geological Survey data release, , doi:10.5066/F7M044MF, 2018.

743 Hausle, D. A. and Coble, D. W.: Influence of sand in redds on survival and emergence of brook
744 trout (Salvelinus fontinalis), Trans. Am. Fish. Soc., 105(1), 57–63, 1976.

745 Hitt, N. P., Snook, E. L. and Massie, D. L.: Brook trout use of thermal refugia and foraging
746 habitat influenced by brown trout, Can. J. Fish. Aquat. Sci., 74(3), 406–418, doi:10.1139/cjfas-
747 2016-0255, 2017.

748 Hudy, M., Thieling, T. M., Gillespie, N. and Smith, E. P.: Distribution, status, and land use
749 characteristics of subwatersheds within the native range of brook trout in the Eastern United
750 States, North Am. J. Fish. Manag., 28(4), 1069–1085, 2008.

751 Irvine, D. J., Lautz, L. K., Briggs, M. A., Gordon, R. P. and Mckenzie, J. M.: Experimental
752 evaluation of the applicability of phase, amplitude, and combined methods to determine water
753 flux and thermal diffusivity from temperature time series using VFLUX 2, J. Hydrol., 531, 728–
754 737, 2015.

755 Isaak, D. J., Young, M. K., Nagel, D. E., Horan, D. L. and Groce, M. C.: The cold-water climate
756 shield: Delineating refugia for preserving salmonid fishes through the 21st century, Glob. Chang.
757 Biol., 21(7), 2540–2553, doi:10.1111/gcb.12879, 2015.

758 Kalbus, E., Reinstorf, F. and Schirmer, M.: Measuring methods for groundwater-surface water
759 interactions: a review, Hydrol. Earth Syst. Sci., 10, 873–887, 2006.

760 Krause, S., Tecklenburg, C., Munz, M. and Naden, E.: Streambed nitrogen cycling beyond the
761 hyporheic zone: Flow controls on horizontal patterns and depth distribution of nitrate and
762 dissolved oxygen in the upwelling groundwater of a lowland river, J. Geophys. Res.
763 Biogeosciences, 118(1), 54–67, doi:10.1029/2012JG002122, 2013.

764 Kurylyk, B. L., Macquarrie, K. T. B., Linnansaari, T., Cunjak, R. A. and Curry, R. A.:
765 Preserving , augmenting , and creating cold-water thermal refugia in rivers : concepts derived
766 from research on the Miramichi River , New Brunswick (Canada), Ecohydrology,
767 1108(October 2014), 1095–1108, doi:10.1002/eco.1566, 2015a.

768 Kurylyk, B. L., MacQuarrie, K. T. B., Caissie, D. and McKenzie, J. M.: Shallow groundwater
769 thermal sensitivity to climate change and land cover disturbances: Derivation of analytical
770 expressions and implications for stream temperature modeling, Hydrol. Earth Syst. Sci., 19(5),
771 2469–2489, doi:10.5194/hess-19-2469-2015, 2015b.

772 Kurylyk, B. L., Irvine, D. J., Carrey, S., Briggs, M. A., Werkema, D. and Bonham, M.: Heat as a
773 hydrologic tracer in shallow and deep heterogeneous media: analytical solution, spreadsheet tool,
774 and field applications, Hydrol. Process., 31(14), 2648–2661, doi:10.1002/hyp.11216, 2017.

775 Leblanc, B. D. R., Massey, A. J., Cochrane, J. J., King, J. H., Smith, K. P. and Survey, U. S. G.:
776 Distribution and Migration of Ordnance- Related Compounds and Oxygen and Hydrogen Stable
777 Isotopes in Ground Water near Snake Pond , Sandwich , Massachusetts , 2001 – 2006, Scientific
778 Investigations Report 2008–5052, , 2001–2006, 2008.

779 LeBlanc, D. R., Guswa, J. H., Frimpter, M. H. and Londquist, C. J.: Ground-water resources of
780 Cape Cod, Massachusetts: U.S. Geological Survey Investigations Atlas HA-692, 4 sheets, 1986.

781 Levy, Z. F., Siegel, D. I., Glaser, P. H., Samson, S. D. and Dasgupta, S. S.: Peat porewaters have
782 contrasting geochemical fingerprints for groundwater recharge and discharge due to matrix
783 diffusion in a large, northern bog-fen complex, J. Hydrol., 541, 941–951,
784 doi:10.1016/j.jhydrol.2016.08.001, 2016.

785 Lowry, C. S., Fratta, D. and Anderson, M. P.: Ground penetrating radar and spring formation in a
786 groundwater dominated peat wetland, J. Hydrol., 373(1–2), 68–79,
787 doi:10.1016/j.jhydrol.2009.04.023, 2009.

788 Luce, C. H., Tonina, D., Gariglio, F. and Applebee, R.: Solutions for the diurnally forced
789 advection-diffusion equation to estimate bulk fluid velocity and diffusivity in streambeds from
790 temperature time series, Water Resour. Res., 49(1), 488–506, doi:10.1029/2012WR012380,
791 2013.

792 MacCrimmon, H. R. and Campbell, S. C.: World Distribution of Brook Trout, Salaelinus
793 fontinalis, J. Fish. Res. Board Canada, 26(1699–1725), 1969.

794 Matthews, K. R. and Berg, N. H.: Rainbow trout responses to water temperature and dissolved
795 oxygen stress in two southern California stream pools, J. Fish Biol., 59, 50–67, 1997.

796 Modica, E.: Source and age of ground-water seepage to streams, USGS Fact Sheet Fact Sheet
797 063-99, 1999.

798 Montgomery, D. R., Buffington, J. M., Peterson, N. P., SchuettHames, D. and Quinn, T. P.:
799 Stream-bed scour, egg burial depths, and the influence of salmonid spawning on bed surface
800 mobility and embryo survival, Can. J. Fish. Aquat. Sci., 53(5), 1061–1070, doi:10.1139/cjfas-53-
801 5-1061, 1996.

802   Mullan, J. W.: The sea run or "Salter" brook trout (Salvelinus fontinalis) fishery of the coastal
803   streams of Cape Cod, Massachusetts, Massachusetts Div. Fish. Game, Bull. 17, 1958.

804   Obruca, W. and Hauer, C.: Physical laboratory analyses of intergravel flow through brown trout
805   redds (Salmo trutta fario) in response to coarse sand infiltration, Earth Surf. Process.
806   Landforms, doi:10.1002/esp.4009, 2016.

807   Petty, J. T., Hansbarger, J. L., Huntsman, B. M. and Mazik, P. M.: Transactions of the American
808   Fisheries Society Brook Trout Movement in Response to Temperature , Flow , and Thermal
809   Refugia within a Complex Appalachian Riverscape Brook Trout Movement in Response to
810   Temperature , Flow , and Thermal Refugia within a Compl, Trans. Am. Fish. Soc., 141(4),
811   1060–1073, doi:10.1080/00028487.2012.681102, 2012.

812   Raleigh, R. F.: Habitat suitability index models: Brook trout., U.S. Dept. Int., Fish Wildl. Serv.,
813   FWS/OBS-82, 1–42, 1982.

814   Rau, G. C., Andersen, M. S., McCallum, A. M., Roshan, H. and Acworth, R. I.: Heat as a tracer
815   to quantify water flow in near-surface sediments, Earth-Science Rev., 129, 40–58,
816   doi:10.1016/j.earscirev.2013.10.015, 2014.

817   Rezanezhad, F., Price, J. S., Quinton, W. L., Lennartz, B., Milojevic, T. and Cappellen, P. Van:
818   Structure of peat soils and implications for water storage , fl ow and solute transport : A review
819   update for geochemists, Chem. Geol., 429, 75–84, doi:10.1016/j.chemgeo.2016.03.010, 2016.

820   Rosenberry, D. O., Briggs, M. A., Delin, G. and Hare, D. K.: Combined use of thermal methods
821   and seepage meters to efficiently locate, quantify, and monitor focused groundwater discharge to
822   a sand-bed stream, Water Resour. Res., 52, 4486–4503, doi:10.1002/2016WR018808, 2016.

823   Seitzinger, S., Harrison, J. a, Böhlke, J. K., Bouwman, a F., Lowrance, R., Peterson, B., Tobias,
824   C. and Van Drecht, G.: Denitrification across landscapes and waterscapes: a synthesis., Ecol.
825   Appl., 16(6), 2064–90 [online] Available from: http://www.ncbi.nlm.nih.gov/pubmed/17205890,
826   2006.

827   Snook, E. L., Letcher, B. H., Dubreuil, T. L., Zydlewski, J., Donnell, M. J. O., Whiteley, A. R.,
828   Hurley, S. T. and Danylchuk, A. J.: Movement patterns of Brook Trout in a restored coastal
829   stream system in southern Massachusetts, Ecol. Freshw. Fish, 26, 360–375,
830   doi:10.1111/eff.12216, 2016.

831   Steel, E. A., Beechie, T. J., Torgersen, C. E. and Fullerton, A. H.: Envisioning, Quantifying, and
832   Managing Thermal Regimes on River Networks, Bioscience, 67(6), 506–522,
833   doi:10.1093/biosci/bix047, 2017.

834   Stoliker, D. L., Repert, D. A., Smith, R. L., Song, B., Leblanc, D. R., Mccobb, T. D., Conaway,
835   C. H., Hyun, S. P., Koh, D., Moon, H. S. and Kent, D. B.: Hydrologic Controls on Nitrogen
836   Cycling Processes and Functional Gene Abundance in Sediments of a Groundwater Flow-
837   Through Lake, Environ. Sci. Technol., 50, 3649–3657, doi:10.1021/acs.est.5b06155, 2016.

838   Walter, B. D. A. and Masterson, J. P.: Simulated Pond-Aquifer Interactions under Natural and
839   Stressed Conditions near Snake Pond , Cape Cod , Water-Resources Investig. Rep. 99-4174, 34,

840   2002.

841   Wehrly, K., Wang, L. and Mitro, M.: Field-based estimates of thermal tolerance limits for trout:
842   incorporating exposure time and temperature fluctuation, Trans. Am. Fish. Soc., 136, 365–374,
843   2007.

844   Winter, T. C., Harvey, J. W., Franke, O. L. and Alley, W. M.: Ground water and surface water; a
845   single resource, Gr. Water U . S . Geol. Surv. Circ. 1139, 79, 1998.

846

847

 Tables

849 Table 1. This table lists 2014 and 2016 drivepoint pore-water chemistry data collected in major

850 streambed groundwater discharge zones located with fiber-optic heat tracing, and in zones of

851 observed repeat trout spawning directly along the bank and farther toward the stream center

852 channel.

open valley groundwater discharges	0.3 m depth		0.6 m depth	
	DO	SpC	DO	SpC
	mg/L	μS/cm	mg/L	μS/cm
GW330	4.6	53.8	4.6	61.3
GW880	1.4	97.7	3.4	65.1
GW1045	0.1	78.8	0.0	82.5
GW1045 (bank)	0.16	105.5	0.39	104.0
GW1045 (channel)	0.31	99.1	0.18	96.4
GW1070	0.2	100.0	0.2	89.8
GW1410	0.0	77.7	0.0	79.0
GW1470	0.1	69.1	0.0	64.3
GW2060	1.4	75.0	0.5	79.4
mean	**0.9**	**84.1**	**1.0**	**80.2**
spawning locations (channel)	0.3 m depth		0.9 m depth	
Spawn 1 channel	4.41	143.9	5.68	143.2
Spawn 2 channel	5.25	139.3	n/a	n/a
Spawn 3 channel	1.76	82.1	2.68	79.9
mean	**3.8**	**121.8**	**4.2**	**111.6**
spawning locations (bank)	0.3 m depth		0.9 m depth	
Spawn 1 bank	7.28	70.6	9.76	55.9
Spawn 2 bank	3.89	70.8	7.17	57.6
Spawn 3 bank (2016)	9.11	60.4	4.91	71.9
Spawn 3 bank (2014)	9.0	56.4	7.6 (0.6 m)	60.9 (0.6 m)
mean	**7.3**	**64.6**	**7.4**	**61.6**

853

854 Table 2. This table lists 2017 drivepoint pore-water chemistry and stable water isotope data

855 collected in a subset of major streambed groundwater seepage zones, zones of observed repeat

856 trout spawning, and from springs located above the water line along the same hillslope as the

857 meander cutbanks of Spawn 1 and Spawn 2.

location	sample depth (m)	SpC (μS/cm)	DO (mg/L)	δ^2H (‰)	$\delta^{18}O$ (‰)	d-xs $\delta^2H - 8* \delta^{18}O$
Hillslope 1	40	74.82	5.004	-51.38	-8.2	**14.22**
Hillslope 2	44	60.59	9.318	-51.81	-8.73	**18.03**
Spawn 1	20	72.45	6.853	-48.9	-7.9	**14.3**
Spawn 2	20	51.75	5.419	-48.2	-7.95	**15.4**
Spawn 3	20	42.62	9.054	-44.32	-7.33	**14.32**
GW1045	20	109.8	0.043	-34.03	-4.93	**5.41**
GW1140	20	103.4	0.043	-32.56	-4.8	**5.84**
GW1470	20	97.68	0.04	-33.05	-4.72	**4.71**

858

859

861
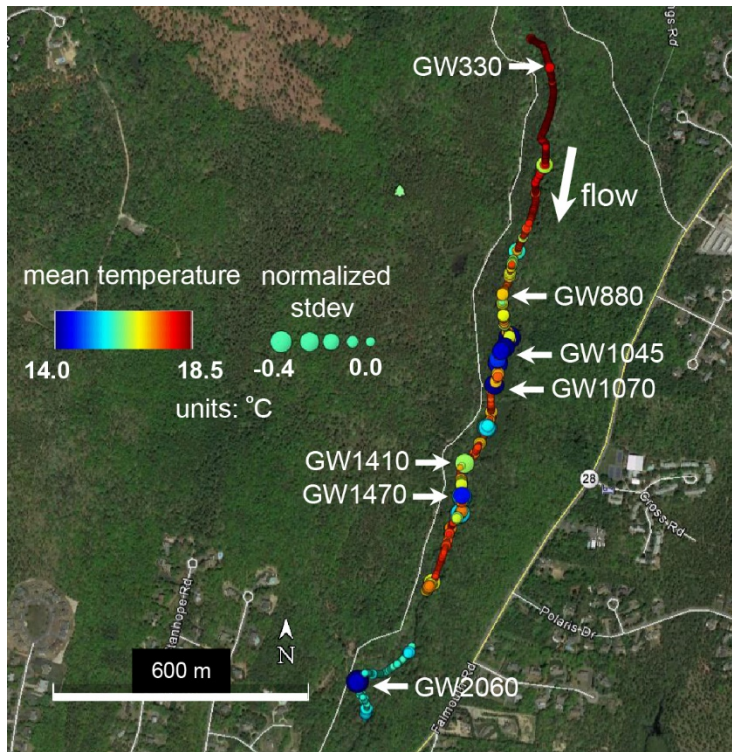
862
863 Figure 1. Fiber-optic distributed temperature data collected along the stream channel sediment-
864 water interface over two days in July 2013 are summarized here using mean temperature (color)
865 and temperature standard deviation normalized to known non-seepage locations (size). Locations
866 of reduced mean temperature and temperature standard deviation can indicate zones of
867 preferential groundwater upwelling. A subset of these apparent upwelling zones (labeled "GW"
868 followed by the distance from upper reach boundary in meters) with varied thermal statistics
869 were chosen for direct pore water sampling and quantitative seepage measurements. This Figure
870 was modified from Rosenberry et al. (2016).

871
872
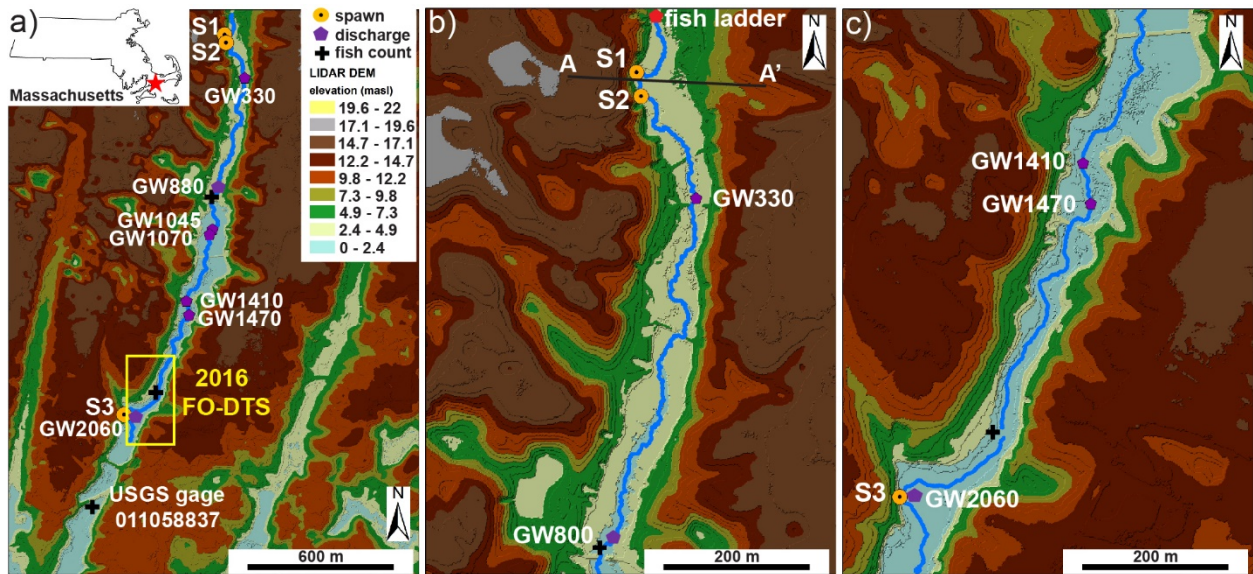
873
874 Figure 2. Lidar elevation data show the linear valley terrain of the Quashnet River study reach, as
875 shown in panel (a) with Spawn (S1, S2, S3) locations and major open valley seepage zones
876 identified. The zoomed in view of panel (b) shows the more narrow upper valley zone where
877 Spawn 1 and 2 are located at the base of a steep cut bank, and the topographic transect of Figure
878 9 (A-A') is noted. Finally, panel (c) displays the lower open valley reach where Spawn 3 is
879 located along a major cut bank.
880

881
882 Figure 3. Several representative images of specific spawn zones and groundwater discharge
883 zones were collected in February 2016. The cut bank alcove at Spawn 1 is shown in panel (a),
884 while the open valley seepage zone GW1045 is shown in (b), and the fresh cut bank slumping
885 and visible seepage at Spawn 3 is shown in (c). Underwater imagery collected at the Spawn 1
886 zone in fall 2015 is displayed in panel (d), showing several fish clustered directly at the base of
887 the cut bank where pore water samples were obtained.
888
889
890
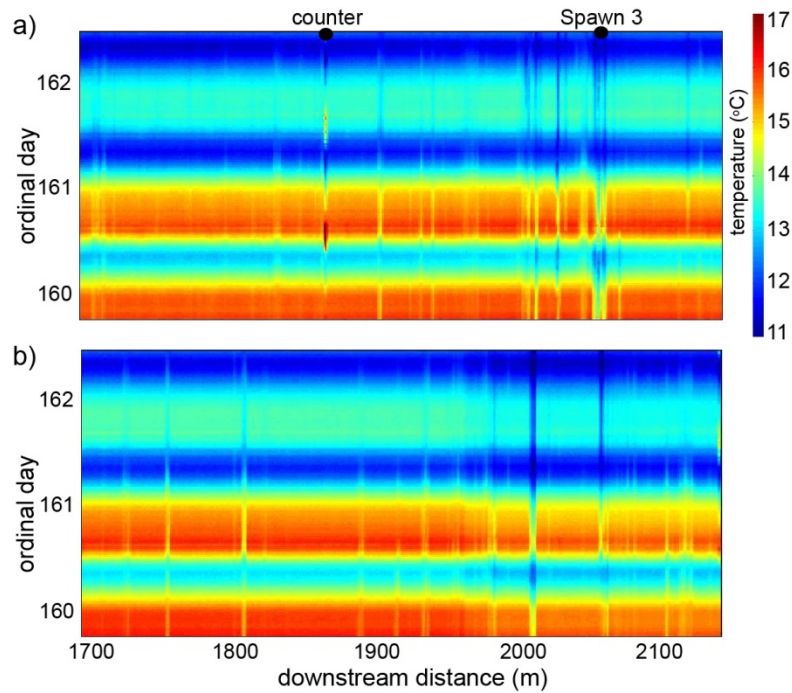
891
892 Figure 4. Fiber-optic-distributed temperature data collected from approximate channel distance
893 1700 to 2160 m along (a) the downstream right bank through the Spawn 3 meander bend area
894 (see Figure 2a for location), and (b) the downstream left bank. The persistent vertical bands of
895 relatively cool temperatures indicate discrete groundwater discharge. Some larger zones display
896 a thermal signature on both bank cables, while smaller discharges may be bank-specific.
897
898
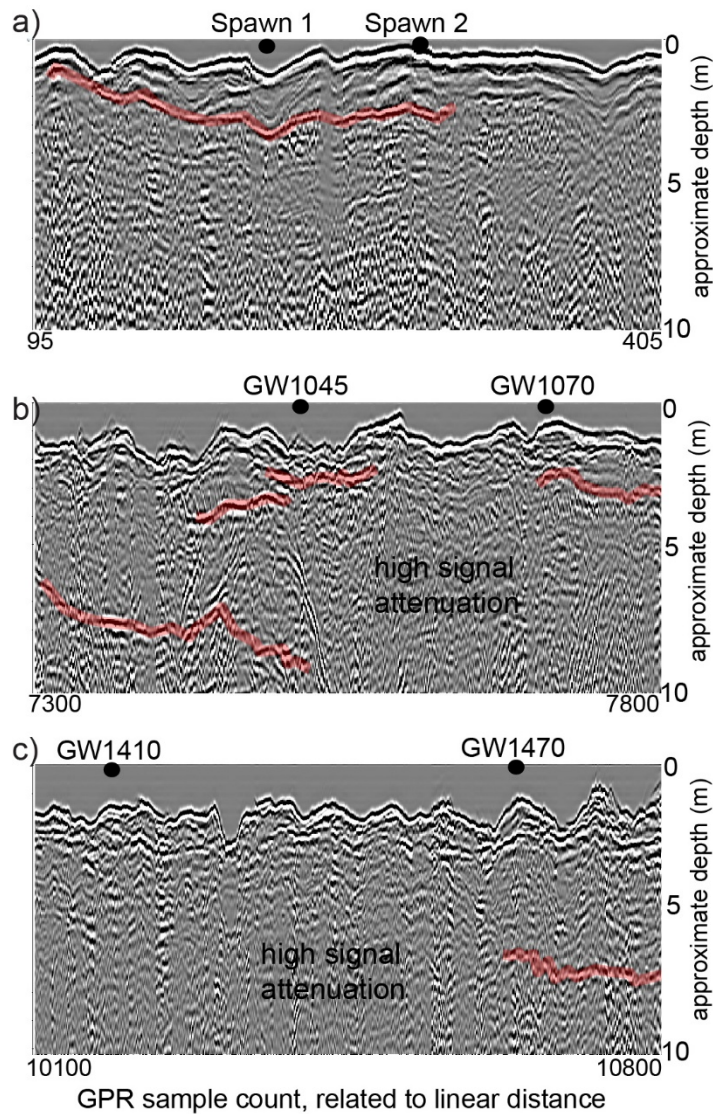
GPR sample count, related to linear distance

Figure 5. These images show ground penetrating radar profiles collected down the center of the river channel to indicate peat and sand/gravel layering in the streambed. Stronger apparent radar reflectors are highlighted in red, and likely indicate sediment layer boundaries (e.g. sand/gravel vs. peat). Spawn and groundwater discharge locations were directly marked in the radar data stream during collection and are shown for each sub-reach panel.
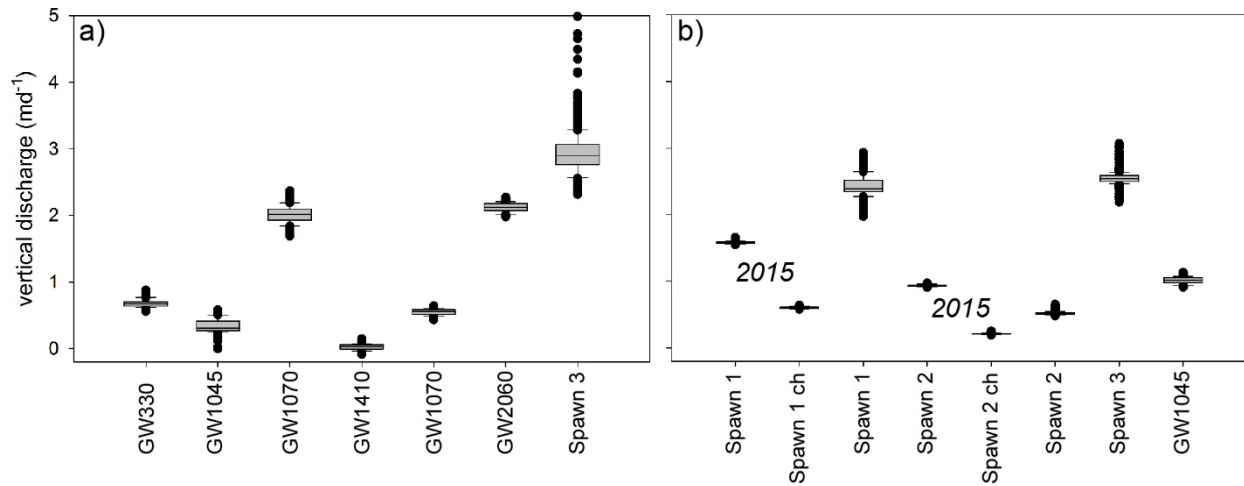
907
908 Figure 6. Summary box plots of sub-daily vertical groundwater discharge rates modeled for the
909 open valley groundwater discharge and Spawn 3 bank locations for the 11 June to 13 July 2014
910 period are shown in panel (a). Additionally, panel (b) shows displays discharge rates collected in
911 Spawn and GW1045 locations directly against the cut banks, and further out towards the channel
912 (indicated by "ch") for the 21 August 21 to 13 September 2015 and 5 June to 9 July 2016
913 periods.
914
915
916
917
918
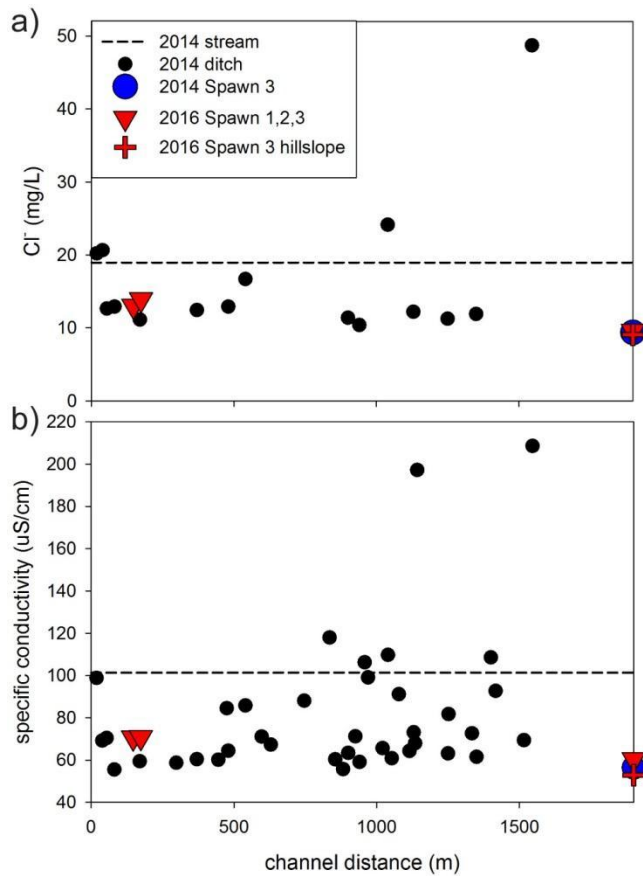
919
920 Figure 7. Drainage ditch chemistry throughout the lower Quashnet showing (a) Cl⁻, and b)
921 specific conductance, collected in June 2014 just above the confluence with the main channel.
922 Data are plotted as distance from the upper flood control structure in the narrow valley reach and
923 compared to groundwater seepage data collected in preferential spawning locations and a
924 hillslope piezometer.
925
926
927
928
929
930
931
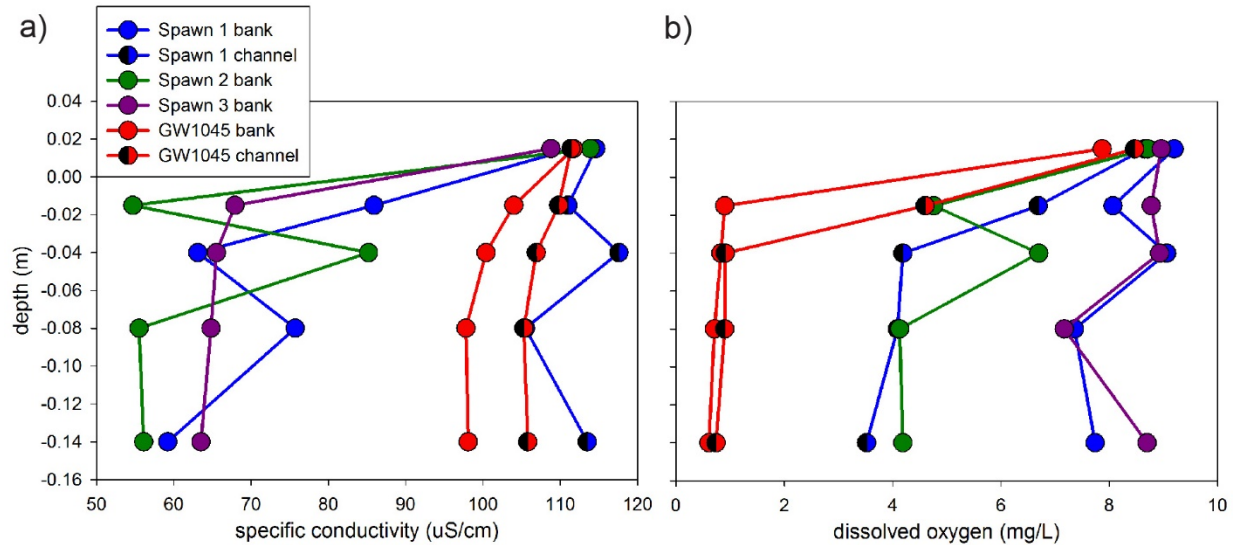
Figure 8. Minipoint pore-water chemistry data showing high spatial resolution profiles of (a) specific conductance, and (b) dissolved oxygen, collected in June 2016 at the major seepage alcoves. Triangle symbols indicate data collected farther toward the thalweg from the respective alcove bank, and all profiles include a local stream water sample taken just above the streambed interface.
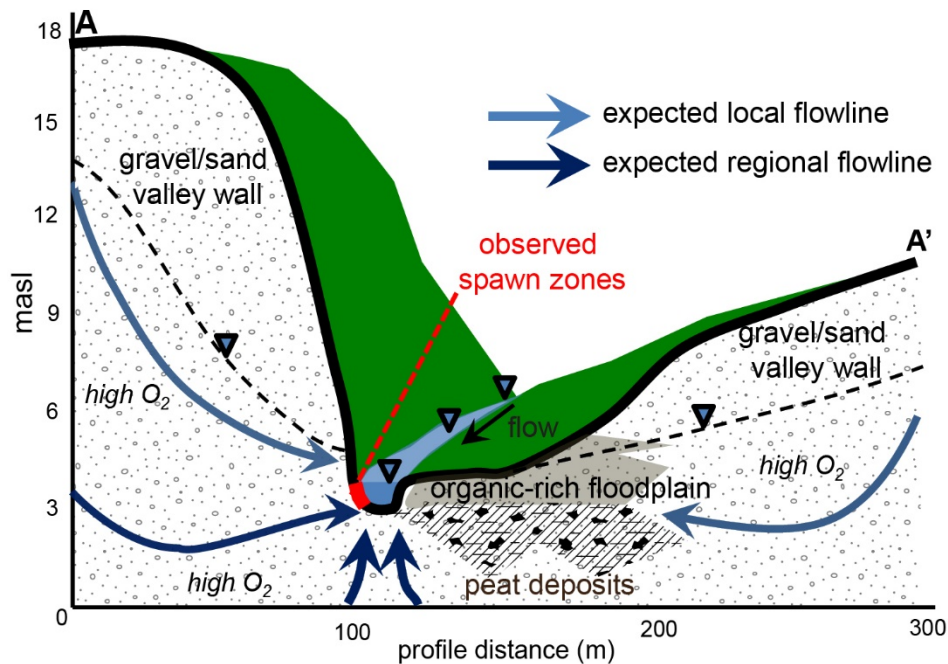
Figure 9. This conceptual model shows how valley wall cutbank discharge zones are likely sourced by locally recharged hillslope groundwaters that avoid substantial interaction with valley floor organic material. The discharging groundwater remains oxygen-rich, therefore supporting trout spawning activity along discrete streambed sections at the meter scale. The topographic profile shown here (A-A') is derived directly from lidar data collected normal to the stream through the Spawn 1 zone, as geolocated in Figure 2b.

Supplemental

948
949   Supplemental Video S1. Underwater video of brook trout spawning in the fall of 2015 (still
950   image Figure 3d).